Journal of Hazardous Materials 193 (2011) 249–256

Contents lists available at ScienceDirect

Journal of Hazardous Materials

journal homepage: www.elsevier.com/locate/jhazmat

Influence of floc size and structure on membrane fouling in coagulation–ultrafiltration hybrid process—The role of Al_{13} species

Weiying Xu, Baoyu Gao*, Ranran Mao, Qinyan Yue

Shandong Key Laboratory of Water Pollution Control and Resource Reuse, School of Environmental Science and Engineering, Shandong University, Ji'nan 250100, Shandong, People's Republic of China

ARTICLE INFO

Article history:
Received 14 April 2011
Received in revised form 9 July 2011
Accepted 14 July 2011
Available online 23 July 2011

Keywords:
Al_{13} species
Coagulation–ultrafiltration
Floc characteristics
Membrane fouling

ABSTRACT

Coagulation application prior to ultrafiltration process was carried out to increase humic acid (HA) removal and membrane permeability. The $[Al_{13}O_4(OH)_{24}(H_2O)_{12}]^{7+}$ polycation (Al_{13} species) was used in the coagulant process and polyaluminum chloride (PACl) was also used for comparison. Characteristics of aggregates pre-coagulated by Al_{13} species and PACl were investigated using a laser diffraction particle sizing device. Additionally, membrane fouling was investigated under different coagulation conditions. The various resistances caused by Al_{13} and PACl treatment effluents were determined using the membrane fouling index equation. The results indicated that at dose of 1 and 3 mg/L, Al_{13} produced larger flocs than PACl; while when dosage further increased, the PACl-HA flocs were much larger. The flocs formed by Al_{13} were strong and compact, and those formed by PACl were weak and loosely structured with the exception of the flocs generated at 1 mg/L. The investigation of membrane fouling demonstrated that Al_{13} contributed to the best effluent permeating at 5 mg/L and the corresponding dose for PACl was 7 mg/L. The adsorption resistance of effluent pre-treated by Al_{13} accounted for a smaller percentage of the total resistances compared with that by PACl.

1. Introduction

Recently, microfiltration (MF) and ultrafiltration (UF) technologies have been used as an alternative to conventional drinking water treatment to meet the requirements of some more stringent regulations [1,2]. UF has been known to be effective for the removal of suspended solids, colloidal material (>0.1 μm), inorganic particulates and fatal microorganisms [3,4]. However, serious fouling of UF membranes and poor removal of dissolved organic matters (DOMs) impeded the widespread application of UF. Addition of a coagulant prior to the membrane filtration has been suggested not only for the purpose of reducing membrane fouling but also improving the removal of DOM that might otherwise not be removed by filtration [5,6]. Choi and Dempsey [7] reported that in line coagulation under under-dosage condition (with respect to conventional treatment) was apparently effective for the removal of natural organic matter (NOM) by ultrafiltration membrane. Barbot et al. [8] showed that coagulation condition and resultant flocs were more important than UF operation condition on membrane fouling for pre-coagulation–UF (C–UF) hybrid process.

Polyaluminum chloride (PACl) was declared superior to traditional aluminum coagulants in removing particulate and/or organic matters in water treatment works [9]. PACl generally contain significant amounts of polynuclear aluminum hydrolysis products, including $Al(OH)_4^-$, $Al(OH)_2^+$, $Al_2(OH)_2^{4+}$, $Al_3(OH)_4^{5+}$, $AlO_4Al_{12}(OH)_{24}(H_2O)_{12}^{7+}$ (Keggin-Al_{13} species) and aluminum hydroxide ($Al(OH)_3$). The Al_{13} species was claimed as the most active species responsible for coagulation [10,11]. In the past several years, much attention has been paid to the removal of natural organic matters (NOMs) by PACl with high content of Al_{13} polymer [12–14]. But the effect of Al_{13} species on membrane process and membrane fouling in C–UF hybrid process has not been completely understood.

Additionally, the floc properties, including floc size, strength and fractal dimension, play an important role in reducing membrane fouling in the C–UF hybrid process. Waite et al. [15] observed a close coupling between the structure and size of hematite flocs formed in suspension and the permeability of the cake layer that accumulated on UF membranes. Lee et al. [16] found that floc structure effects were more significant for smaller floc, with higher specific resistance for cakes formed from more compact flocs. Barbot et al. [8] reported that the effect of coagulation on the permeate flux depended on the ability of flocs resisting to shear stress. Thus the study of floc properties is essentially meaningful for water treatment by C–UF hybrid process.

* Corresponding author. Tel.: +86 531 88364832; fax: +86 531 88364513.
E-mail address: baoyugao_sdu@yahoo.com.cn (B. Gao).

0304-3894/$ – see front matter © 2011 Elsevier B.V. All rights reserved.
doi:10.1016/j.jhazmat.2011.07.057

The main objective of the present paper was to investigate the influence of Al_{13} species on NOM removal efficiency and membrane fouling in C–UF hybrid process. In addition, the size, strength and fractal structure of aggregates formed by Al_{13} species were described in detail and the effect of various characteristics of formed flocs on the different resistances of membrane fouling was subsequently evaluated.

2. Materials and methods

2.1. Water samples

Humic acid (HA) is ubiquitous in surface water and is the major organic constituent of drinking water [17]. Hence it is necessary and meaningful to study the removal of HA in water treatment works.

HA used in this study was obtained as a commercial reagent grade solid (Shanghai, China). The HA stock solution was prepared as follows: 1.0 g of HA was dissolved in deionized water that contained 4.2 g of $NaHCO_3$ and then the solution was diluted to 1 L. The synthetic test water was prepared by dissolving 10.0 mL of HA stock solution with deionized water to 1 L. The property of this synthetic test water was as following: $UV_{254} = 0.217 \pm 0.03$, DOC = 3.84 ± 0.05 mg/L, pH = 8.25 ± 0.1.

2.2. Preparation and characterization of coagulants

PACl and Al_{13} species were used as the coagulants in all the tests. PACl was synthesized by adding 12.72 mg of Na_2CO_3 and 28.97 mg of $AlCl_3{\cdot}6H_2O$ slowly into 100 mL of deionized water under intense agitation. The temperature was kept at 70.0 ± 0.5 °C by using recycling water bath [18]. Al_{13} species was separated from the PACl by ethanol/acetone separation method. Specifically, 10 mL of PACl solution was transferred into a 1 L glass beaker, and then 50, 100 and 50 mL of ethanol–acetone solution was introduced into the PACl solution in sequence under gentle agitation. Samples were filtered using 0.45 μm millipore membranes at the end of each addition of ethanol–acetone solution. The precipitates obtained by the second filtration were dried at room temperature, which was the expected Al_{13} species. All the reagents used to prepare each coagulant were of analytical grade and deionized water was used to make all solutions.

Total Al content in PACl was determined by titrimetric method according to the National Standard of China [19]. The Al species in PACl and Al_{13} polymer were analyzed by ^{27}Al nuclear magnetic resonance (NMR) spectroscopy with ^{27}Al NMR spectra obtained from a Varian UNITY INOVA (500 MHz). Sample was placed in 5 mm tubes and the spectra generated at 20 °C. Standard solutions of given monomeric Al concentration were run using a coaxial sample tube, with a 0.2 M Na aluminate solution in the inner insert as reference. The intensities for ^{27}Al signals relative to the aluminate reference were used for calculating the corresponding signals of Al concentration. There are three signals in the NMR spectra: the signal near 0.0 ppm represents the monomeric and dimeric aluminum species (denoted as Al_m); the signal at 62.5 ppm represents the Al_{13} species; and the signal at 80.0 ppm indicates the formation of $Al(OH)_4^-$ (the internal standard). Based on the contents of Al_m and Al_{13} species, the other Al species (denoted as Al_{other}) can be calculated by the following equation:

$$Al_{other} = Al_T - Al_m - Al_{13} \quad (1)$$

The properties of coagulants used in this study were summarized in Table 1.

Table 1
The concentrations and Al species distributions of PACl and Al_{13} polymer.

Coagulant	Al_T (mol/L)	Al_m (%)	Al_{13} (%)	Al_{other} (%)
PACl	1.080	34.26	24.83	40.91
Al_{13} polymer	0.096	4.73	91.64	3.63

2.3. Coagulation experiments and on-line measurement of floc size

Coagulation experiments were initially conducted by variable speed jar test apparatus (ZR4-6, Zhongrun Water Industry Technology Development Co. Ltd., China) with 50 mm × 40 mm flat paddle impellers and 1 L cylindrical beakers. The sample was rapidly mixed up by shear rate at 200 revolutions per minute (rpm) for 30 s initially and then a certain dose of coagulant was added, with simultaneously 1.5 min of rapid mixing at 200 rpm again. After that, the sample was exposed to a slow mixing at 40 rpm for 15 min, followed by 20 min of settlement period to allow the aggregated flocs to settle down. After sedimentation, the water sample was carefully withdrawn by syringe from about 3 cm below the water surface and passed through a 0.45 μm glass filter paper for analysis. UV_{254} absorbance at 254 nm wavelength was tested using an UV-754 UV/vis spectrophotometer (Precision Scientific Instrument Co. Ltd., Shanghai, China). An unfiltered sample was obtained after the rapid mix for zeta potential measurement using a Zetasizer 3000HSa (Malvern Instruments, UK).

A continuous laser diffraction instrument (Mastersizer 2000, Malvern, UK) was used to measure the dynamic flocs size as the coagulation proceeded. The suspended floc was monitored through the optical unit of the Mastersizer and transferred back into the jar by a peristaltic pump (LEAD-1, Longer Precision Pump, China) with a 5 mm internal diameter tube. The size measurements were taken every 30 s for the duration of the jar test. More detail has been reported in other paper [20].

2.4. Floc strength and fractal structure

In this study, a floc breakage mode was used to indicate the floc strength. The breakage experiments were performed using the experimental setup similar to those of Jarvis et al. [21]. The aggregated flocs after each flocculation were exposed to increased shear force at 50, 75, 100, 150, 200 and 300 rpm for a further 5 min. Dynamic floc size during breakage under each level of shear force was monitored and the rate at which a floc suspension decayed under exposure to shear was indicative of the strength of the flocs within the system as the steady-state floc size was governed by the prevailing stress conditions within the containing vessel. Previous studies revealed the relation on a log–log scale between the average velocity gradients G in the flocculation and the floc size of the suspension in equilibrium [22,23]:

$$\lg d = \lg C - \gamma \lg G \quad (2)$$

where d is the floc diameter; C is the floc strength constant that strongly depends on the method used for particle size measurement; G is the average velocity gradient and γ is the stable floc size exponent dependent upon floc break-up mode. The slope of the line (γ) gives an indication of the rate of degradation. A larger γ value is indicative of floc that is more prone to break into smaller size under an increasing shear force. In this instance, the rpm was used instead of the G and an adapted version of Eq. (2) was used as shown below:

$$\lg d = \lg C' - \gamma' \lg \mathrm{rpm} \quad (3)$$

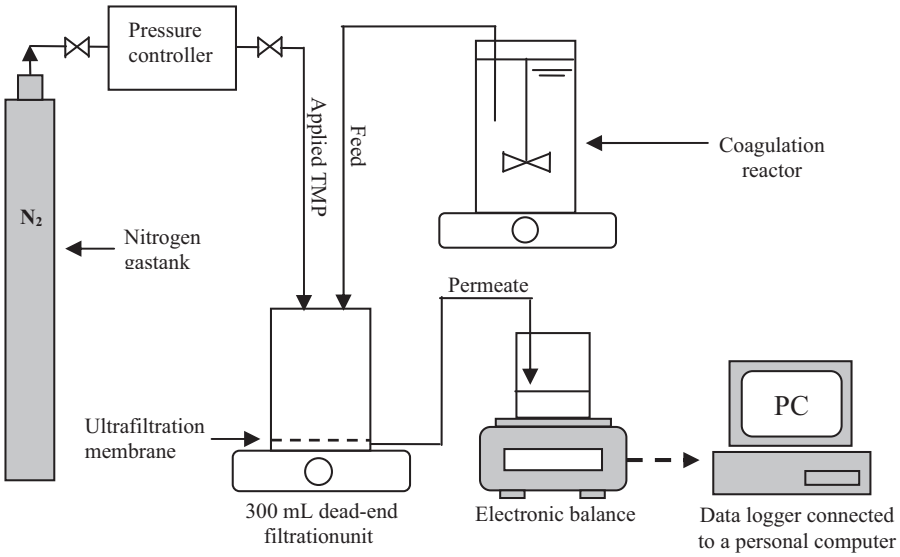

Fig. 1. Schematic diagram of the coagulation and dead-end ultrafiltration test setup.

where C' is the modified floc strength constant, rpm is the revolutions per minute on the jar tester and γ' is a fitting coefficient.

Floc fractal dimension was determined using light scattering experiments and described by the following relationship between the measured scattered intensity of aggregate clusters ($I(q)$) and the momentum transfer (q):

$$I(q) \propto q^{-D_f} \quad (4)$$

The power relationship in Eq. (4) is confirmed by plotting I against q on a log–log scale. If this yields a straight line, the power law relationship exists and the slope of the line is D_f. The D_f indicates the mass fractal scaling relationship within the aggregates and the D_f value demonstrates the degree of floc compaction. Compact aggregates have higher D_f values, while aggregates with loose structures have lower D_f.

2.5. Ultrafiltration procedure

The ultrafiltration experiments were conducted using a dead-end batch ultrafiltration unit with a 300 mL-capacity stirred cylindrical beaker. Schematic diagrams of the experimental setup for the dead-end C–UF hybrid process were shown in Fig. 1. After coagulation, the suspension was allowed to settle quiescently for 20 min. And then, the coagulation effluent solution was gently decanted from the coagulation tank to the dead-end filtration unit and filtered through ultrafiltration membrane (Mosu, China) with cut-off molecular weight (MWCO) of 100 kDa. Stirring was maintained in the ultrafiltration stirred cell to keep the suspension homogeneous and to prevent flocs from settling. However, the stirring velocity was kept low in order to prevent flocs breakage. The membrane material was polyethersulfone (PES) and the effective membrane area was 50.24 cm^2. A fresh piece of membrane was used in every experiment. Prior to the filtration of coagulation suspension, the membrane was "wetted" to its optimal operating condition. Nitrogen gas was used to maintain precise supply of constant pressure at 180 kPa. Instantaneous mass of cumulative permeate was measured by electronic balances (MSU5201S-000-D0, SARTORIUS AG GERMANY) which was recorded via a personal computer equipped with a data acquisition system.

3. Results and discussion

3.1. Removal of humic acid

Initially, the effect of coagulant dose on HA removal in the pre-coagulation–UF hybrid unit was investigated by performing a series of jar tests. The HA removal efficiency and zeta potentials under various coagulant doses were shown in Figs. 2 and 3, respectively. When the dose was less than 7 mg/L, the removal efficiency increased dramatically with dose for both PACl and Al_{13} species. When the dose further increased, the growth of removal efficiency by Al_{13} species was obstructed and even decreased when the sample water was pre-treated by PACl. It should be noted that at the dose of 1 mg/L, Al_{13} species obviously contributed to better efficiency of HA removal than PACl. This could be attributed to the stable structure [20] and better charge neutralization ability of Al_{13} polymer as shown in Fig. 3, which enabled the Al_{13} species to destabilize the HA molecules and form fine particles even at very low dose. And then, the formed aggregates could easily be removed by the filtration membrane. By comparison, PACl gave rise to higher

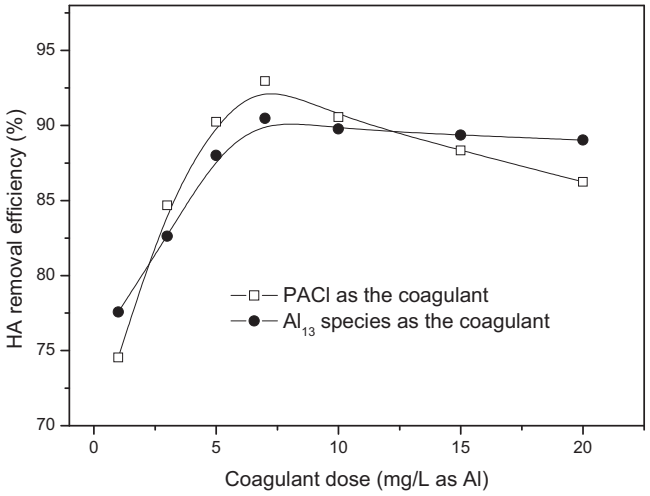

Fig. 2. Removal of HA by coagulation–ultrafiltration process under different aluminum-based coagulants and doses.

Table 2
Floc breakage rates for PACl and Al_{13} coagulants at various doses.

Coagulant	Dosage (mg/L)					
	1	3	5	7	10	
PACl	γ'	0.37	0.80	0.74	0.71	0.78
	R^2	0.99	0.96	0.97	0.97	0.97
Al_{13}	γ'	0.76	0.69	0.61	0.65	0.67
	R^2	0.97	0.98	0.96	0.97	0.98

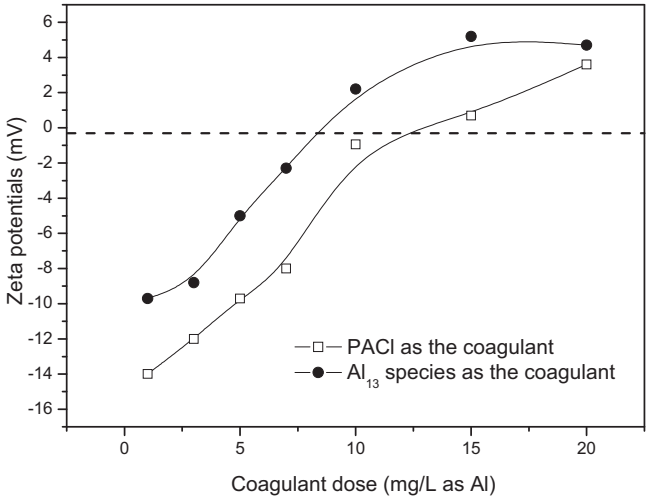

Fig. 3. Zeta potential under different aluminum-based coagulants and doses.

removal efficiency at the medium dose of 3–7 mg/L. At high coagulant concentration (higher than 7 mg/L), HA removal efficiency decreased obviously for PACl and Al_{13} contributed to almost invariable efficiency at high dose. This demonstrated that further increase in coagulant dose would no longer be helpful and even had negative effect on HA removal in the C–UF process.

3.2. Floc size

The growth of flocs throughout the coagulation under different coagulant doses were studied and considering the efficiency of HA removal by the C–UF processes, the coagulant dose was fixed in the low and medium range (1–10 mg/L). The 50 percentile floc size ($d_{0.5}$), which was obtained through the measurement of the laser diffraction instrument, was used to denote floc size in this study. The results were shown in Fig. 4. It could be found that in all cases, floc size increased rapidly with coagulation time during the first several minutes, followed by a gentle growth and finally reached a plateau, which has been generally regarded as a result of equilibrium between floc formation and floc breakage [24]. The floc steady-state size increased with coagulant dose for both Al_{13} polymer and PACl coagulants. Specifically, the floc formed by Al_{13} at 7 mg/L and 10 mg/L reached almost the same size at the steady state, which means that the charge reversal restricted the floc growth at dose of 10 mg/L. At dose of 1 mg/L, the stable Al_{13} floc reached a $d_{0.5}$ size of 250 μm and the floc size increased to nearly 310 μm at dosage of 3 mg/L. By comparison, PACl produced flocs with much smaller size, which were only around 80 μm at 1 mg/L and 250 μm at 3 mg/L. However, the aggregates formed by PACl became larger than those formed by Al_{13} as dose increased. The bridging or/and adsorption of organic matters onto amorphous precipitates in PACl coagulation substantially increased the floc size [12].

3.3. Floc strength and fractal structure

In order to investigate the floc strength under different coagulation conditions, the flocs which had reached the steady-state were exposed to increased shear. When the floc size after 5 min exposure to high shear was plotted against *G*-value, a straight line could be drawn through the data ($R^2 > 0.95$) on a log-log scale as shown in Fig. 5. It was observed that the floc size decreased intensely as shear force increased and the responses to the increasing shear were similar for PACl and Al_{13} polymer. However, the decreasing rates of floc size were dependent on the characteristics of coagulants and doses.

To quantitatively compare the differences of PACl and Al_{13} in response of floc d_{50} to increased shear, the slopes of the decreasing lines (γ' values) were calculated according to Fig. 5 and listed in Table 2. For PACl, the flocs presented a surprisingly low γ' value of 0.37 at dose of 1 mg/L, which indicated a gentle slope of the floc decrease line. This suggested that the flocs were strong and with good ability to resist the increased shear forces. In the dose range of 3–7 mg/L, the flocs were much weaker than those formed at dose of 1 mg/L but were getting stronger with the dose increasing.

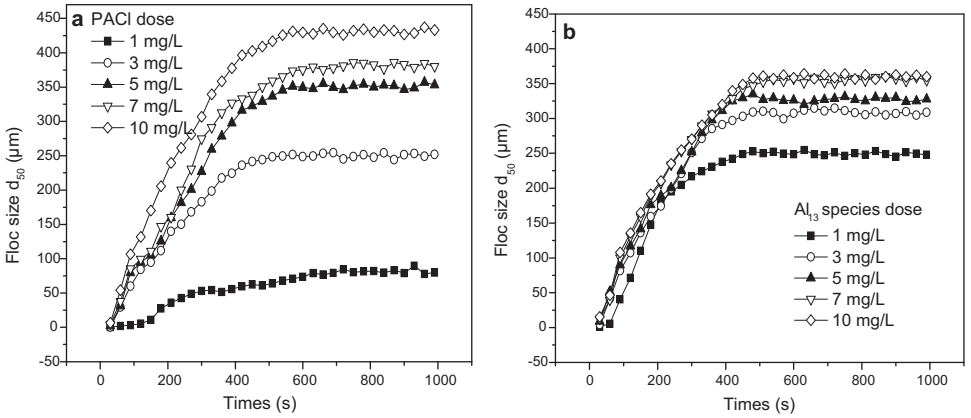

Fig. 4. Variations of floc size during coagulation by (a) PACl and (b) Al_{13} polymer under different doses (■ 1 mg/L, ○ 3 mg/L, ▲ 5 mg/L, ▽ 7 mg/L, ◊ 10 mg/L).

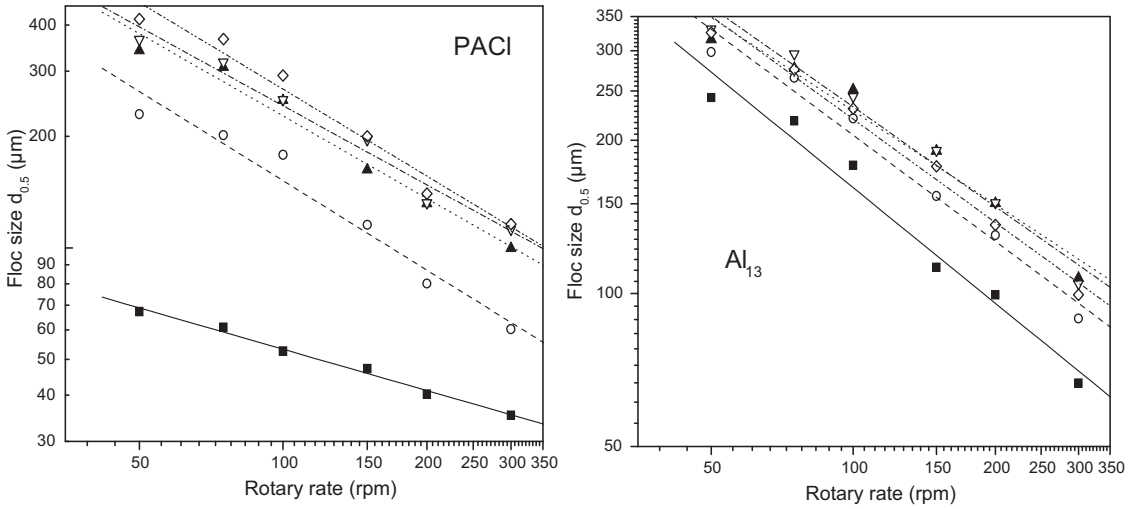

Fig. 5. Effect of different shear forces on floc size for PACl and Al_{13} coagulants under different doses (■ 1 mg/L, ○ 3 mg/L, ▲ 5 mg/L, ▽ 7 mg/L, ◊ 10 mg/L).

The increasing dose induced less charge repulsion and thus facilitated the formation of strong aggregates. And when the dose continuously increased to 10 mg/L, the flocs became weaker again according to the higher γ' value of 0.78.

The influence of Al_{13} species on the floc strength could also be learned from the data shown in Table 2. Unlike the results for PACl coagulation, the γ' of flocs formed by Al_{13} species decreased initially and then increased with dosage, which indicated that there existed an optimum dose that gave rise to the strongest flocs. In this study, the lowest γ' value was obtained at dose of 5 mg/L (0.61) and this was the result of both charge neutralization and the aggregates size. When coagulant concentration increased in the range of 1–5 mg/L, floc strength improved with the decreasing charge repulsion. When the dosage further increased to 10 mg/L, charge reversion occurred but the floc size increased continuously. It should be noted that, the γ' obtained at 7 mg/L was larger than that at 5 mg/L although the dose at 7 mg/L contributed to less charger repulsion. This was due to the larger floc size produced at 7 mg/L than 5 mg/L. The larger aggregates could be more affected by the microscale eddies which resulted in floc breakage. At small sizes, flocs were more likely to be entrained within eddies rather than be broken by them [24]. Consequently, the floc strength was impaired by the increasing sizes. This was also the reason why PACl-HA flocs at 1 mg/L presented high degree of strength with the γ' value of only 0.37 while 10 mg/L contributed to weak flocs with γ' value of 0.78.

It is worth noticing that Al_{13} species contributed to stronger flocs in a wide dose range of 3–10 mg/L compared to PACl. This could be ascribed to the Al_{13} aggregates with more branches [10], which also contributed to more physical bonds and subsequently strengthened the resultant flocs. Another reason was also associated with the larger steady floc size formed by PACl than Al_{13} polymer.

The fractal dimensions of flocs during different coagulation time were measured according to Eq. (4) and presented in Table 3. It could be found that lower dosage tended to give rise to flocs with higher D_f values no matter which coagulant was used. Flocs formed by Al_{13} polymer were with higher D_f in the dose range investigated in this study, implying that the Al_{13}-HA flocs were more compact than PACl-HA flocs. It was due to the fact the higher positive charge of Al_{13} polymer greatly weakened the repulsive forces between particles within the aggregates and hence, led to a high degree of compaction. The breakage of flocs could definitely improve the compact degree of flocs based on the varying degrees of increases in D_f values of flocs after breakage under different coagulation conditions. This agreed with the current understanding that flocs become more compact under exposure to increasing shear as they break at their weak points and rearrange into more stable and tight structures [25].

Table 3
Floc fractal dimensions (D_f) for PACl and Al_{13} coagulants at various doses.

Coagulant	Dosage (mg/L)				
	1	3	5	7	10
Before breakage					
PACl	2.17	2.32	2.36	2.28	2.23
Al_{13}	2.41	2.47	2.45	2.38	2.30
After breakage					
PACl	2.29	2.35	2.37	2.30	2.29
Al_{13}	2.46	2.53	2.51	2.43	2.39

3.4. Membrane performance

The normalized membrane permeate fluxes of effluents coagulated by PACl and Al_{13} polymer were investigated at different dosages (1, 3, 5, 7 and 10 mg/L). Fig. 6 exhibited the size distributions of coagulation effluents, which were exactly the feed water of ultrafiltration. The results indicated that Al_{13} resulted in feed water with smaller $d_{0.5}$ values than PACl. The crucial reason was the high strength of Al_{13}-HA flocs and better ability to resist tiny eddies in the system as shown in Table 2.

The normalized fluxes associated with filtration time were presented in Fig. 7. As can be seen, in all cases, the fluxes decreased dramatically first and then the declines became inconspicuous, where the fluxes were relatively steady. However, a significant difference of flux variation was observed when the suspension was pre-coagulated under different conditions. For PACl, the most severe flux decline occurred in system with the coagulant concentration of 1 mg/L. When the dose increased from 3 to 7 mg/L, the severity of flux decline reduced. This could be ascribed to the improvement of floc strength, which was not likely to be destroyed and left less aggregates fractions in the feed water. This could also be proved by the results displayed in Fig. 6a, which demonstrated a reduction of volume percentage of large size (>100 μm) and a decrease in the $d_{0.5}$ size with dosage in the range of 3–7 mg/L. The flux at coagulant dose of 10 mg/L was lower than that at dose of 7 mg/L. This was also caused by the higher value of γ' at 10 mg/L, indicating that the aggregates were easier to be broken by the turbulence flow and/or microscale eddies in the coagulation system and the desquamated fragments would promote the formation of cake layer, and subsequently the flux decline was aggravated.

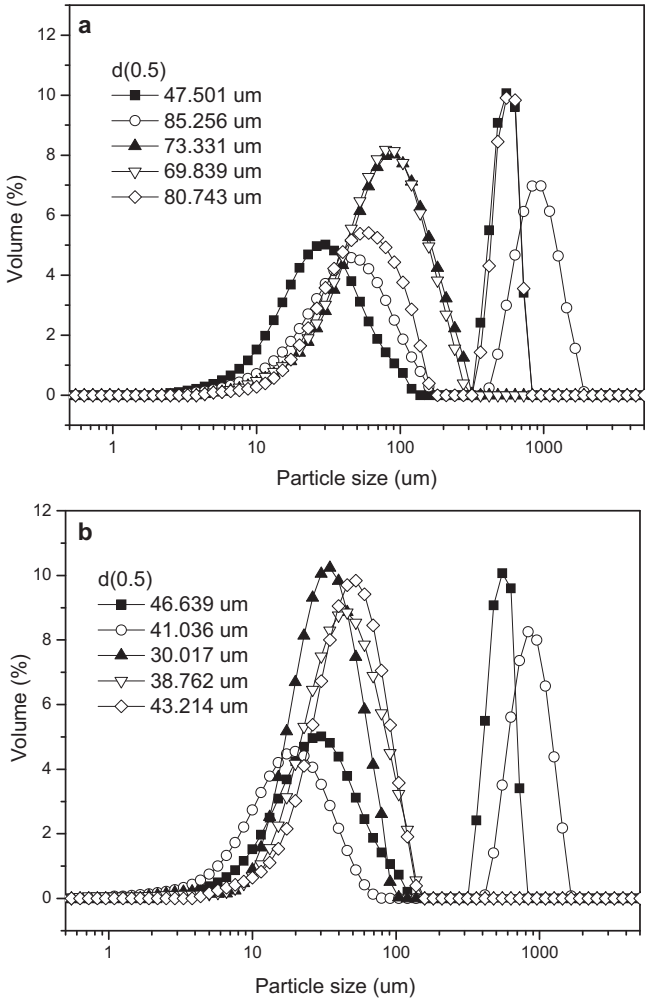

Fig. 6. Size distribution of the feed water of ultrafiltration membrane treated by (a) PACl and (b) Al_{13} polymer at different coagulant dosages (■ 1 mg/L, ○ 3 mg/L, ▲ 5 mg/L, ▽ 7 mg/L, ◊ 10 mg/L).

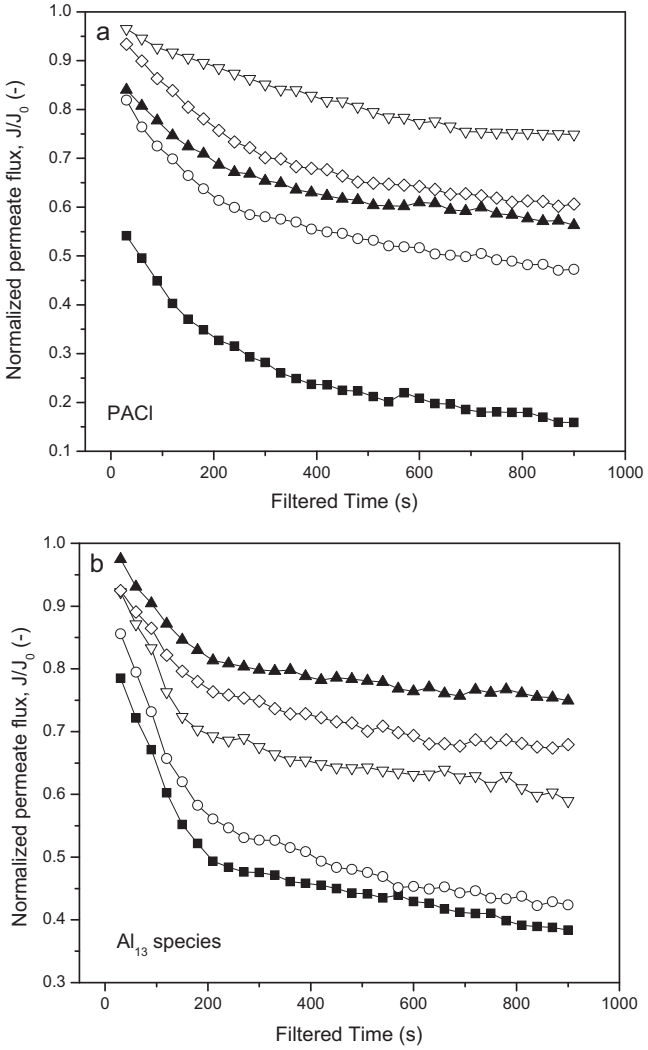

Fig. 7. Normalized flux decline of systems containing various doses of PACl and Al_{13} species. Feed solutions were prepared by the jar tests in Section 2.1. Operating conditions: 20 °C feed solution, TMP 180 kPa and pH 7.0 (■ 1 mg/L, ○ 3 mg/L, ▲ 5 mg/L, ▽ 7 mg/L, ◊ 10 mg/L).

Another point worth noticing is that the flux at dosage of 1 mg/L was the lowest even though the flocs formed at dose of 1 mg/L had high strength. This was due to the small size of original flocs formed at 1 mg/L. Small aggregates settled slowly and part of them remained in the effluent and then impeded the permeation of suspension.

The flux declines caused by effluents coagulated with Al_{13} species were quite different. As shown in Fig. 7b, the severity of flux decline increased in the following order: 5 mg/L < 10 mg/L < 7 mg/L < 3 mg/L < 1 mg/L. According to the results shown in Table 2, the flocs formed at dose of 5 mg/L had the highest strength and the feed water had the lowest $d_{0.5}$ size (Fig. 6b). As a result, the flux declined most slightly. It should be pointed out that the severity of permeate flux seemed consistent with the sequence of floc strength on the whole, which was in agreement with the results of PACl coagulated effluents. However, the normalized permeate flux for Al_{13} at 7 mg/L was lower than that at 10 mg/L even though the flocs formed at 7 mg/L was stronger than those formed at 10 mg/L. This was due to the different floc fractal structures. It has been stated that compact flocs with larger D_f lead to high level of resistance to ultrafiltration, while the loosely structured aggregates with lower D_f produce less resistance and thus are beneficial for membrane permeability [26]. Based on the data in Table 3, the flocs formed at 7 mg/L were more compact with the D_f of 2.38; while the D_f of flocs generated at 10 mg/L was 2.30. And the result did not change after the breaking of generated flocs. Thus the remaining flocs in effluent for 7 mg/L led to compact cake layer with high resistance than that for 10 mg/L.

3.5. Resistance analysis

To further observe how the HA floc properties produced by PACl and Al_{13} species affected the membrane fouling, a series of analyses were conducted in this study to calculate the various resistances generated by different effluents. Resistances due to different fouling mechanisms were determined according to the Resistance in Series Model [27] as follows:

$$J = \frac{\Delta P}{\eta(R_m + R_a + R_p + R_c)} \quad (5)$$

where J is permeate flux, ΔP is trans-membrane pressure (defined as the difference between the applied pressure and the osmotic pressure), η is dynamic viscosity, and R denotes the resistance: R_m is membrane hydraulic resistance, R_a is resistance due to adsorption, R_p is resistance caused by pore blocking and R_c is resistance due to cake layer. The calculation methods and the corresponding equations of various resistances were listed in Table 4 according to the experimental procedures.

Table 4
Calculation of different resistances during filtration process.

Steps	Resistance	How measured	Corresponding equation
1	R_m	DI water was filtered through virgin membrane for at least 2 h	$R_m = \frac{\Delta P}{\eta J_0}$ (6) where J_0 is the permeate flux of DI water filtered through the clean membrane
2	R_a	The same membrane was immersed in the coagulation effluent for 18 h; DI water was filtered through the "fouled" membrane for another 2 h	$R_a = \frac{\Delta P}{\eta J'} - R_m$ (7) where J' denotes the steady permeate flux of DI water filtered through the "soaked" membrane at the end of filtration
3	R_t	The coagulation effluent was filtered through the same membrane for at least 2 h	$R_t = \frac{\Delta P}{\eta J}$ (8) where J is the relatively steady permeate flux of coagulation effluent through the membrane at the end of filtration
4	R_p	The fouled membrane was gently wiped with Kimwipes to remove the cake layer on the surface, and DI water was filtered once again through the membrane for 2 h	$R_p = \frac{\Delta P}{\eta J''} - R_m - R_a$ (9) where J'' is the steady permeate flux of DI water through the membrane at the end of filtration
5	R_c	Subtract all other resistances to the total resistance	$R_c = R_t - R_m - R_a - R_p$ (10)

The results of this analysis verified that the membrane resistances in this study consisted of resistance due to the membrane, the formation of cake layer and the adsorption. The resistance caused by pore blocking according to other papers [6,28] was almost zero. The investigated resistances were plotted in the percentage-relative to the total resistance and the results were shown in Fig. 8.

For PACl coagulation effluent, the low coagulant dose (1 mg/L) gave the largest R_a and R_c percentages of the total resistance. This was caused by the small aggregates that remained in the suspension (Fig. 6a), which were difficult to precipitate as aforementioned. It could also be observed that the resistances caused by adsorption and cake layer reduced markedly as the dose increased slightly from 1 to 3 mg/L which was due to the significant growth of flocs. The large aggregates were better able to settle and as a consequence, much less flocs remained in the effluent except a few fragments broken off from the large aggregates. As visually observed, the proportions of R_a in the total resistances were in the following hierarchy: 1 mg/L > 3 mg/L > 10 mg/L > 5 mg/L > 7 mg/L. It was observed that this sequence was the very reverse of the floc strength order except in the case of 1 mg/L. Stronger flocs formed during coagulation led to lower R_a proportion, which was mainly attributed to the fewer aggregate fractions left in the effluent. However, it seemed that the R_c did not match the floc strength hierarchy because the floc fractal structure also had a distinct effect on the R_c. Choi et al. [29] reported that flocs of high humic water, small and with high fractal dimension, gave rise to higher specific cake resistance. At PACl dose of 5 mg/L, the resultant flocs were the most compact with the D_f value of 2.37. Consequently, the associated R_c reached the largest proportion of the total resistance except the case of 1 mg/L.

When Al_{13} polymer was used as the coagulant, the various resistances distributions in the total resistances were quite different from those for PACl. The most obvious difference was the change of proportion of resistances caused by adsorption and cake layer. At dose of 1 mg/L, both the R_a and R_c proportions were apparently lessened in comparison with those for PACl. This was because the preformed Al_{13} polymer was stable in the suspension and could play an active part by way of charge neutralization in coagulation unit [20]. As a result, the effluent

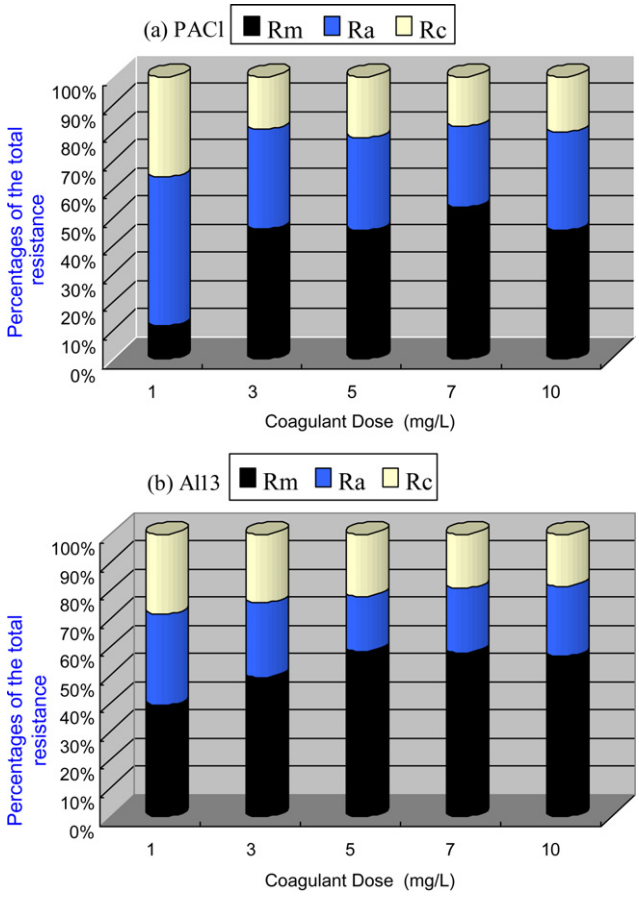

Fig. 8. Proportions of various resistances analysis of the effluents coagulated by (a) PACl and (b) Al_{13} species. R_a, R_c and R_m denote the resistances caused by adsorption, cake layer and membrane hydraulic resistance, respectively.

was cleaner and produced less adsorption and cake layer resistances. Under different Al_{13} doses, the R_a proportions decreased in the following order: 1 mg/L > 3 mg/L > 10 mg/L > 7 mg/L > 5 mg/L. The results demonstrated the same conclusion as that for PACl, which implied that the R_a mainly depended on the strength of generated flocs. Compared with PACl, Al_{13} polymer was inclined to produce stronger flocs in dose range of 3–10 mg/L (Table 2). As a result, the proportion of R_a relative to the total resistance for Al_{13} coagulation effluent was remarkably smaller than that for PACl coagulation effluent. However, the evaluation of R_c was dependent on both the floc strength and fractal structure. The results in Table 3 indicated that Al_{13} polymer was inclined to produce denser flocs with larger D_f values than PACl. Thus, if by any chance the generated aggregates segments remained in the effluent, the compact floc fractions would deposit on the surface of the ultrafiltration membrane and produced a compact cake layer, which led to higher proportion of R_c. So Al_{13} polymer did not appear to be conducive to the diminution of R_c.

4. Conclusions

The results of this study suggested that Al_{13} species displayed distinct influence on characteristics of HA aggregates from PACl and had different impacts on the membrane fouling. The experimental conclusions were mainly as follows.

(1) At doses of 1–3 mg/L, pre-hydrolyzed Al_{13} species contributed to larger flocs than PACl, while with coagulant dose further increasing, the flocs formed by PACl were obviously larger than those formed Al_{13} polymer.
(2) Except in the case of 1 mg/L, Al_{13} polymer produced stronger and more compact aggregates than PACl in the coagulation dose range investigated in this study. Additionally, Al_{13} contributed to the strongest aggregates at dose of 5 mg/L and the most compact flocs at 3 mg/L; while the corresponding doses for PACl were 7 and 10 mg/L, respectively.
(3) The optimum coagulation dose of Al_{13} with respect to the membrane permeability was 5 mg/L and for PACl was 7 mg/L. Effluent coagulated by Al_{13} species presented lower proportion of R_a in the total resistance due to the high strength of Al_{13}-HA flocs, but this did not work in the case of R_c due to the high D_f of Al_{13}-HA flocs.

Acknowledgements

The research was supported by Specialized Research Fund for the Doctoral Program of Higher Education (No. 20070422019), the National Natural Sciences Foundation of China (Nos. 50678095, 50808114), the Key Projects in the National Science & Technology Pillar Program in the Eleventh Five-year Plan Period (No. 2006BAJ08B05) and the National Major Special Technological Programmes Concerning Water Pollution Control and Management in the Eleventh Five-year Plan Period (No. 2008ZX07422-003-02). The kind suggestions from the anonymous reviewers are highly appreciated.

References

[1] S.J. Judd, P. Hillis, Optimisation of combined coagulation and microfiltration for water treatment, Water Res. 35 (2001) 2895–2904.
[2] C. Guigui, J.C. Rouch, B. Durand, L.V. Bonnelye, P. Aptel, Impact of coagulation conditions on the in-line coagulation/UF process for drinking water production, Desalination 147 (2002) 95–100.
[3] C. Jucker, M.M. Clark, Adsorption of aquatic humic substances on hydrophobic ultrafiltration membrane, J. Membr. Sci. 96 (1995) 137–152.
[4] A.W. Zularisam, A.F. Ismail, R. Salim, Behaviours of natural organic matter in membrane filtration for surface water—a review, Desalination 194 (2006) 211–231.
[5] T. Carroll, S. King, S.R. Gray, B.A. Bolto, N.A. Booker, The fouling of microfiltration membranes by NOM after coagulation treatment, Water Res. 34 (11) (2000) 2861–2868.
[6] J.D. Lee, S.H. Lee, M.H. Jo, P.K. Park, C.H. Lee, J.W. Kwak, Effect of coagulation conditions on membrane filtration characteristics in coagulation–microfiltration process for water treatment, Environ. Sci. Technol. 34 (17) (2000) 3780–3788.
[7] K.Y. Choi, B.A. Dempsey, In-line coagulation with low-pressure membrane filtration, Water Res. 38 (2004) 4271–4281.
[8] E. Barbot, S. Moustier, J.Y. Bottero, P. Moulin, Coagulation and ultrafiltration: understanding of the key parameters of the hybrid process, J. Membr. Sci. 325 (2008) 520–527.
[9] H.X. Tang, Z.K. Luan, Features and mechanism for coagulation flocculation processes of polyaluminum chloride, J. Environ. Sci. 7 (1995) 204–211.
[10] J.Y. Bottero, J.M. Cases, F. Fiessinger, J.E. Poirier, Studies of hydrolyzed aluminum chloride solutions. 1. Nature of aluminum species and composition of aqueous solutions, J. Phys. Chem. 84 (1980) 2933–2939.
[11] C.Z. Hu, H.J. Liu, J.H. Qu, D.S. Wang, J. Ru, Coagulation behavior of aluminum salts in eutrophic water: significance of Al_{13} species and pH control, Environ. Sci. Technol. 40 (2006) 325–331.
[12] H. Zhao, C.Z. Hu, H.J. Liu, X. Zhao, J.H. Qu, Role of aluminum speciation in the removal of disinfection byproduct precursors by a coagulation process, Environ. Sci. Technol. 42 (2008) 5752–5758.
[13] M.Q. Yan, D.S. Wang, J.H. Qu, W.J. He, C.W.K. Chow, Relative importance of hydrolyzed Al(III) species (Al_a, Al_b, and Al_c) during coagulation with polyaluminum chloride: a case study with the typical micro-polluted source waters, J. Colloid Interface Sci. 316 (2007) 482–489.
[14] X.H. Wu, D.S. Wang, X.P. Ge, H.X. Tang, Coagulation of silicamicrospheres with hydrolyzed Al(III)—significance of Al_{13} and Al_{13} aggregates, Colloids Surf. A 330 (2008) 72–79.
[15] T.D. Waite, A.I. Schafer, A.G. Fane, A. Heuer, Colloidal fouling of ultrafiltration membranes: impact of aggregate structure, J.Colloid Interface Sci. 212 (1999) 264–274.
[16] S.A. Lee, A.G. Fane, R. Amal, T.D. Waite, The effect of floc size and structure on specific cake resistance and compressibility in dead-end microfiltration, Sep. Sci. Technol. 38 (2003) 869–887.
[17] J.L. Lin, C. Huang, C.J.M. Chin, J.R. Pan, The origin of $Al(OH)_3$-rich and Al_{13}-aggregate flocs composition in PACl coagulation, Water Res. 43 (2009) 4285–4295.
[18] B.Y. Gao, Z.J. Zhang, J.W. Ma, X.Y. Cao, Solid–solid mixed method to prepare polyaluminum chloride, Environ. Chem. 24 (2005) 569–572 (in Chinese).
[19] GB15892-1995, Water Treatment Chemicals-Polyaluminum Chloride, National Standards of the People's Republic of China (in Chinese).
[20] Y. Wang, B.Y. Gao, X.M. Xu, W.Y. Xu, G.Y. Xu, Characterization of floc size, strength and structure in various aluminum coagulants treatment, J. Colloid Interface Sci. 332 (2009) 354–359.
[21] P. Jarvis, B. Jefferson, S.A. Parsons, Breakage, regrowth, and fractal nature of natural organic matter flocs, Environ. Sci. Technol. 39 (2005) 2307–2314.
[22] S.B. Francois, Strength of aluminum hydroxide flocs, Water Res. 21 (1987) 1023–1030.
[23] A.K. Yeung, R. Pelton, Micromechanics: a new approach to studying the strength and breakup of flocs, J. Colloid Interface Sci. 184 (1996) 579–585.
[24] P. Jarvis, B. Jefferson, J. Gregory, S.A. Parsons, A review of floc strength and breakage, Water Res. 39 (2005) 3121–3137.
[25] C. Selomulya, R. Amal, G. Bushell, T.D. Waite, Evidence of shear rate dependence on restructuring and break-up of latex aggregates, J. Colloid Interface Sci. 236 (2001) 67–77.
[26] J. Wang, J. Guan, S.R. Santiwong, T.D. Waite, Characterization of floc size and structure under different monomer and polymer coagulants on microfiltration membrane fouling, J. Membr. Sci. 321 (2008) 132–138.
[27] A.I. Schafer, A.G. Fane, T.D. Waite, Nanofiltration—Principles and Applications, 1st ed., Elsevier Advanced Technology, Oxford, 2005.
[28] J. Wang, J. Guan, S.R. Santiwong, T.D. Waite, Effect of aggregate characteristics under different coagulation mechanisms on microfiltration membrane fouling, Desalination 258 (2010) 19–27.
[29] Y.H. Choi, S. Han, J.H. Kim, Y. Kweon, Role of hydrophobic natural organic matter flocs on the fouling in coagulation-membrane processes, Sep. Purif. Technol. 62 (2008) 529–534.